DNA breaks are key contributors to the cost of antibiotic resistance

Roberto Balbontín*[, 1, 2] and Isabel Gordo*[, 1]

[1] Instituto Gulbenkian de Ciência; Oeiras, 2780-156; Portugal

[2] Lead Contact

* Correspondence: rbalbontin@igc.gulbenkian.pt, igordo@igc.gulbenkian.pt

Summary

Antibiotic resistance often causes a fitness cost to bacteria in the absence of the drug. The cost is the main determinant of the prevalence of resistances upon reducing antibiotics use. Understanding its causes is considered the Holy Grail in the antibiotic resistance field. We show that most of the variation in the cost of resistances common in pathogens can be explained by DNA breaks, a previously unsuspected cause. We demonstrate that the cost can be manipulated by targeting the RNase responsible for degrading R-loops, which cause DNA breaks. Indeed, lack of RNase HI drives resistant clones to extinction in populations with high initial frequency of resistance. Thus, RNase HI provides a promising target for antimicrobials specific against resistant bacteria, which we validate using a repurposed drug. These results show previously unknown effects of resistance on bacterial physiology and provide a framework for the development of new strategies against antibiotic resistance.

Keywords

antibiotic resistance; fitness cost; DNA breaks; RNase HI targeting; repurposed drug.

Introduction

Antibiotic resistance entails a large human and economic burden worldwide (*Global antimicrobial resistance surveillance system (GLASS) report: Early implementation 2017-2018. Geneva: World Health Organization. 2018*). Its maintenance and spread in bacterial populations depend on the rate at which resistance is acquired and on its effect on bacterial fitness. This effect is typically deleterious, resulting in the so-called cost of resistance. The cost of resistance is influenced by the environment, by interactions between the resistances and the genetic background in which they appear (epistasis), and by subsequent acquisition of mutations compensating for fitness defects (compensatory evolution) (Durão, Balbontín, & Gordo, 2018). Importantly, the magnitude of the cost is the main biological parameter influencing the fate of resistances upon reducing antibiotic use (Dan I. Andersson & Hughes, 2010). Despite its importance, the causes of the cost are far from being completely understood (Vogwill & MacLean, 2015), and the identification of these causes has become the “Holy Grail” in the antibiotic resistance field.

Resistance mutations often map to genes encoding proteins targeted by antibiotics. These target proteins are typically involved in essential functions, such as transcription, translation, DNA replication or cell wall biosynthesis. Resistance mutations cause alterations in the structure of the target protein, rendering it insensitive to the drug, but often adversely affecting its function (Andersson & Levin, 1999, Andersson & Hughes, 2010, Durão, Balbontín, & Gordo, 2018). These pleiotropic effects hold the key to manipulating resistance levels in bacterial populations (Dan I. Andersson & Hughes, 2010).

Rifampicin and streptomycin resistance mutations (Rif^R and Str^R), common in pathogenic bacteria, map to the genes *rpoB* and *rpsL*, encoding the β' subunit of the RNA polymerase and the 30S ribosomal subunit protein S12, respectively. Rif^R and Str^R mutations are representative examples of resistances to antibiotics targeting transcription and translation, respectively. Rif^R mutations show different costs (Jin & Gross, 1989, Reynolds, 2000), and these are commonly attributed to alterations in the rates of transcription initiation, elongation, slippage or termination (Guarente & Beckwith, 1978, Das, Merril, & Adhya, 1978, Yanofsky & Horn, 1981, Gowrishankar & Pittard, 1982, Fisher & Yanofsky, 1983, Hammer, Jensen, Poulsen, Oppenheim, & Gottesman, 1987, Jin, Walter, & Gross, 1988, Jin *et al.*, 1988, Jin & Gross, 1989, Jin & Gross, 1991, Zhou & Jin, 1997, Zhou & Jin, 1998, Reynolds, 2000, Zhou *et al.*, 2013). Likewise, most Str^R mutations also cause a cost (Ruusala, Andersson, Ehrenberg, & Kurland, 1984, Schrag & Perrot, 1996, Paulander, Maisnier-Patin, & Andersson, 2009), which is currently interpreted via the effects of these mutations on translation fidelity and processivity (Gorini & Kataja, 1964, Gartner & Orias, 1966, Ozaki, Mizushima, & Nomura, 1969, Birge & Kurland, 1969, Galas & Branscomb, 1976, McMahon & Landau, 1982, Bohman, Ruusala, Jelenc, & Kurland, 1984, Dong & Kurland, 1995, Schrag & Perrot, 1996, Paulander, Maisnier-Patin, & Andersson, 2009). Thus, at present, the costs of Rif^R and Str^R mutations are thought to be caused by defects in protein synthesis, either at a global cellular level (Applebee, Herrgård, & Palsson, 2008, Hall, 2013, Qi, Preston, & MacLean, 2014) or limited to specific functions or regulons (Zhou & Jin, 1998, Paulander, Maisnier-Patin, & Andersson, 2009, Ochi & Hosaka, 2013, Pelchovich *et al.*, 2014).

Motivated by the principle that compensatory evolution would be capable of shedding light on the evolutionary cause of the cost of resistance, we recently showed that the fitness cost of double resistance (Rif^R Str^R) can be reduced via overexpression of *nusG* or *nusE* (Moura de Sousa, Balbontín, Durão, & Gordo, 2017), which encode the proteins that physically connect the RNA polymerase and the ribosome (Burmann *et al.*, 2010). This suggests that the reduction of the cost can be achieved by reinforcing the coupling between transcription and translation, besides the already known partial recovery in protein biosynthesis (Andersson & Hughes, 2010). Coupling between transcription and translation is known to prevent spontaneous backtracking of the RNA polymerase (Herbert *et al.*, 2010, Proshkin, Rahmouni, Mironov, & Nudler, 2010, Kohler, Mooney, Mills, Landick, & Cramer, 2017, Saxena *et al.*, 2018), which can ultimately cause double-strand DNA breaks (Dutta *et al.*, 2011). This led us to hypothesize that cells carrying different Rif^R and Str^R mutations have higher number of DNA breaks, and it is the DNA breaks that drive their cost.

In this study, we show that DNA breaks caused by resistance mutations are major contributors to their fitness cost, explaining 73% of its variation across resistant genotypes. The involvement of R-loops in the generation of DNA breaks allowed us to identify RNase HI as an important determinant of the cost of resistance, which we validate using a repurposed drug. We further show that targeting RNase HI is a plausibile strategy for the effective eimination of resistant bacteria, as lack of RNase HI favors extinction of resistant clones when competing against sensitive bacteria, abolishing compensatory evolution.

Results

DNA breaks explain variation in the fitness cost of resistance

In order to test if Rif^R and Str^R mutations generate DNA breaks, and whether DNA breaks drive the cost of resistance, we simultaneously measured competitive fitness and activation of the SOS response (Maslowska, Makiela-Dzbenska, & Fijalkowska, 2019), a well-known proxy for the occurrence of DNA breaks (Quillardet, Huisman, D'Ari, & Hofnung, 1982). We carried out these assays in sensitive *E. coli*, Str^R strains ($RpsL^{K43N}$, $RpsL^{K43T}$, and $RpsL^{K43R}$), Rif^R strains ($RpoB^{H526L}$, $RpoB^{H526Y}$, and $RpoB^{S531F}$), and double resistant mutants carrying the nine possible combinations of these resistance alleles. Remarkably, fourteen out of the fifteen resistant strains show increased SOS activation (Figure 1A), demonstrating that resistance mutations indeed cause DNA breaks. Moreover, the SOS induction strongly correlates with the cost of resistance, explaining 73% of its variation (Figure 1B). This suggests that DNA breaks are key contributors to the cost of resistance. To independently confirm the occurrence of DNA breaks in resistant bacteria, we used a system which permits direct visualization of double-stranded DNA ends by fluorescence microscopy (Shee *et al.*, 2013). We combined this system with the SOS reporter, and analyzed a subset of resistant mutants and sensitive bacteria. As expected, this corroborated that resistance mutations indeed cause increased number of DNA breaks (Table 1, Figure S1). We then asked if resistance mutations involving a different mechanism which could lead to perturbations of transcription-translation coupling also generate DNA breaks. The commonly used antibiotic erythromycin targets the 50S ribosomal subunit,

affecting translation and its coupling with transcription (Sedlyarova *et al.*, 2017). Erythromycin resistance mutations (Erm^R) mapping to the genes *rplD* and *rplV* (encoding the 50S ribosomal subunit proteins L4 and L22, respectively) are known to reduce translation elongation rate (Chittum & Champney, 1994, Zaman, Fitzpatrick, Lindahl, & Zengel, 2007), likely affecting transcription-translation coupling. We isolated Erm^R clones carrying either $RplD^{G66R}$ or $RplV^{\Delta(82-84)}$ mutations and found that both mutants show increased SOS (Figure 1C), demonstrating that other resistance mutations, with a different mechanistic basis but affecting the same process (transcription-translation coupling) also cause DNA breaks.

The cost of resistance can be very reduced when bacteria grow in glucose as the sole carbon source, and specific Rif^R and/or Str^R alleles show no significant cost in such minimal medium (Paulander, Maisnier-Patin, & Andersson, 2009, Trindade, Sousa, & Gordo, 2012, Durão, Trindade, Sousa, & Gordo, 2015). We therefore reasoned that, if DNA breaks are an important cause of the cost, they should be reduced in an environment where the costs are smaller. In agreement with our hypothesis, resistant mutants show reduced DNA breaks in minimal medium (Figure 2A), leading to and a weaker correlation between DNA breaks and the cost (Figure 2B). This further validates DNA breaks as a key predictor of the fitness cost of antibiotic resistance.

Compensatory evolution cause reduction of DNA breaks

We then hypothesized that, if DNA breaks are major drivers of the fitness cost of resistance, compensatory evolution of resistant strains should result in a reduction of DNA breaks. To test this, we compared the cost and SOS induction in the RpsL^{K43T} RpoB^{H526Y} double mutant and in an isogenic strain additionally carrying the most prevalent compensatory mutation found in our previous study: RpoC^{Q1126K} (Moura de Sousa *et al.*, 2017). As hypothesized, both cost and SOS induction are greatly reduced in the compensated strain (Figure 3A), confirming that DNA breaks are targeted by compensatory evolution. In order to test if this is general, we analyzed nine compensated clones from three independent populations of the RpsL^{K43T} RpoB^{H526Y} double mutant propagated for fifteen days in the absence of antibiotics. As expected, the costs are smaller in the evolved strains and, as hypothesized, all the nine compensated clones show decreased SOS induction compared to their resistant ancestor (Figure 3B). This demonstrates that compensatory evolution widely targets mechanisms that reduce DNA breaks and further reinforces the notion that DNA breaks are major contributors to the cost of antibiotic resistance.

RNAse HI strongly influences the fitness of resistant bacteria

Transcription-translation uncoupling leads to increased formation of R-loops, which cause DNA breaks (Dutta *et al.*, 2011). We thus reasoned that the increased number of DNA breaks in the resistant mutants could also involve R-loops. In this scenario, deleting RNase HI, which specifically degrades R-loops (Tadokoro & Kanaya, 2009), should lead to increased DNA breaks and greater costs of Rif^{R} and Str^{R}. Accordingly, both DNA breaks and the cost of resistance are greatly exacerbated in the *ΔrnhA*

168 background (Figure 4A, Table 1, Figure S2, Figure S3A). Conversely, mild overproduction of RNase
169 HI can ameliorate both phenotypes in a subset of mutants (Figure S4); however, strong overproduction
170 is toxic for the cell (Stockum, Lloyd, & Rudolph, 2012, Wimberly *et al.*, 2013), irrespectively of its
171 genotype (Figure S5). These results confirm the involvement of R-loops in the uncoupling-mediated
172 production of DNA breaks caused by resistance and suggest that RNase HI can be a target for
173 manipulating the fitness of resistant strains.
174
175 RNase HI can serve as a target specific against resistant bacteria
176
177 We then asked whether targeting RNase HI function could be used to select specifically against
178 resistant bacteria in polymorphic populations with high frequency of resistance. RNase HI inhibitors
179 are currently studied as antiretrovirals (Tramontano, Corona, & Menendez-Arias, 2019). A
180 commercially available one, RHI001, has been shown to inhibit the activity of purified *E. coli* RNase
181 HI protein *in vitro* (Kim *et al.*, 2013). In competitions between sensitive and resistant bacteria, we
182 observed that addition of RHI001 to the medium increases the cost of most resistant mutants (Figure
183 4B), on average by 14%. RHI001 also reduces fitness of double resistant bacteria more than that of
184 sensitive bacteria in the absence of competition (Figures S3B and S3C). Chemical inhibition was not as
185 effective as genetic removal (which increases cost on average by 28%) (Figure 4C and D), as may be
186 expected, since stability, diffusibility across the bacterial envelope, pharmacokinetics and
187 pharmacodynamics of RHI001 *in vivo* are unknown, and potentially suboptimal. Nevertheless, these
188 results suggest that inhibiting RNase HI may be a plausible strategy to select specifically against

resistant strains coexisting with sensitive bacteria, as long as resistant strains fail to evolve adaptations that abrogate their extinction. In order to test this hypothesis, we propagated a mixture of sensitive bacteria (CFP-labeled) competing against a pool of five single resistant mutants (YFP-labeled RpsL^{K43N}, RpsL^{K43T}, RpoB^{H526L}, RpoB^{H526Y}, and RpoB^{S531F}) during 15 days, in the absence of antibiotics. We studied the frequency dynamics of resistant clones under both strong bottlenecks (1:1500 dilutions), where new adaptive mutations are less likely to spread, and weak bottlenecks (1:50 dilutions), where propagation of adapted clones is more probable. In parallel, we performed identical propagations, but in which all strains lack RNase HI, as a proxy for optimal inhibition of RNase HI function. We observed that, in the presence of RNase HI, sensitive bacteria initially outcompete resistant clones but, as the propagation progresses, resistant bacteria increase in frequency - likely due to compensatory evolution - finally reaching coexistence (Figure 5A, blue lines). Remarkably, in the propagations of strains lacking RNase HI, resistant bacteria were completely outcompeted and went extinct by day seven (Figure 5A, red lines), even under mild bottlenecks (Figure 5B). Altogether, these results show that targeting RNase HI is a promising strategy to selectively eliminate resistant bacteria.

Discussion

We show that mutations known to affect protein synthesis generate DNA breaks, which explain 73% of the variation in their cost (Figure 1, Table 1, Figure S1). Compensatory evolution indicates that these resistances cause uncoupling between transcription and translation (Moura de Sousa *et al.*, 2017), which can result in DNA breaks (Dutta, Shatalin, Epshtein, Gottesman, & Nudler, 2011). Indeed, we

show that the RpsL^{K43N} RpoB^{H526Y} and RpsL^{K43T} RpoB^{H526Y} double mutants, which combine alleles that cause increased transcription elongation rate (Fisher & Yanofsky, 1983) and decreased translation rate (Schrag & Perrot, 1996, Hosaka *et al.*, 2004), show the highest costs and DNA breaks (Figure 1). Curiously, inhibition of translation has been shown to alleviate the cost of Rif^{R} mutations in *Pseudomonas aeruginosa* (Alex R. Hall, Iles, & MacLean, 2011). In light of the results presented here, this observation is compatible with a scenario in which Rif^{R} mutations cause a perturbation of transcription-translation coupling by virtue of reduced RNA polymerase processivity, and translation inhibitors promote re-coupling by decreasing ribosomal activity. In agreement with the notion of single resistance mutations causing significant uncoupling, single Rif^{R} or Str^{R} mutationswith high cost (Trindade *et al.*, 2009) cause a strong induction of the SOS response (Figure S6A). We also showed that RNase HI is a key determinant of the fitness of resistant mutants (Figure 4, Table 1, Figure S3A, Figure S4). Interestingly, transcription-translation uncoupling caused by chemical inhibition of translation can generate R-loops (Broccoli *et al.*, 2004, Dutta, Shatalin, Epshtein, Gottesman, & Nudler, 2011, Negro *et al.*, 2019). Thus, perturbations of the coupling between transcription and translation increases the requirement of RNase HI function by bacteria. This opens the possibility to designing novel therapeutic interventions by combining drugs targeting transcription or translation with RNase HI inhibitors in order to increase DNA breaks and costs of resistance, therefore enhancing the effectiveness of antimicrobial treatments.

DNA breaks induced by transcription-translation uncoupling involve increased replication-transcription conflicts (Dutta *et al.*, 2011), which have been shown to cause both R-loops (Lang *et al.*,

2017) and DNA breaks (Merrikh *et al.*, 2012). We observed more DNA breaks in rich than in minimal media (Figure 1A, Figure 2A). This might be linked to the fact that replication-transcription conflicts are maximized during fast replication (Merrikh, Machón, Grainger, Grossman, & Soultanas, 2011), and bacteria replicate faster in rich than in minimal media (C. H. Wang & Koch, 1978) (Figure S6B). Supporting this notion, we observed that, in rich medium, the costs are detected in the first 4 hours, when cells are growing exponentially, while resistant bacteria can even show advantage when growth slows down (Figure S6C). Consistent with this observation, resistant mutants have been shown to outcompete sensitive bacteria in aging colonies (Wrande, Roth, & Hughes, 2008, Katz & Hershberg, 2013). Another interesting fact is that stable DNA replication (initiation of DNA replication at sites different from *OriC*) can be induced by lack of RNase HI or conditions that activate SOS (Kogoma, 1997). Thus, Rif^R and Str^R mutations, which induce SOS, could favor replication-transcription conflicts via induction of stable DNA replication. This can generate a feed-forward loop of synergistic deleterious effects, which may be further enhanced by the downregulation of *rnhA* caused by the induction of the SOS response (Quiñones, Kücherer, Piechocki, & Messer, 1987). This detrimental runaway loop and the environmental effects on the cost described above could potentially be exploited therapeutically, via concurrent chemical and dietary treatments designed to maximize the cost of resistance.

We revealed RNase HI as a promising target specific against resistant bacteria (Figure 4), and showed that lack of RNase HI favors extinction of resistant clones, preventing compensatory evolution (Figure 5). This is specially important for resistances mediated by mutations (Hershberg, 2017) or for

pathogens that acquire antibiotic resistance exclusively through mutation, such as *Mycobacterium tuberculosis*, which often carries Rif^R and Str^R mutations (Almeida Da Silva & Palomino, 2011). Interestingly, RNase HI has been proposed as an antimycobacterial target due to its essentiality in *Mycobacterium smegmatis* (Minias *et al.*, 2015, Gupta, Chatterjee, Glickman, & Shuman, 2017). The results presented here support the plausibility of this strategy.

An understanding of the determinants of maintenance and dissemination of antibiotic resistance, such as its cost, is urgently needed (*Global antimicrobial resistance surveillance system (GLASS) report: Early implementation 2017-2018. Geneva: World Health Organization. 2018*). We show that DNA breaks drive the cost of resistance and reveal RNase HI as a promising antimicrobial target specific against resistant bacteria, which we validated using a repurposed drug. Overall, our results uncover important effects of resistances on bacterial physiology and demonstrate the plausibility of exploiting these effects to develop novel strategies against antibiotic resistance.

Acknowledgments

The authors thank Professor Susan M. Rosenberg and Dr. Christian J. Rudolph for kindly providing bacterial strains, the Flow Cytometry and Advanced Imaging facilities of Instituto Gulbenkian de Ciência for technical assistance, Miguel Godinho for useful discussions, and Karina Xavier, Leonardo Gastón Guilgur, Pol Nadal Jiménez and the members of the Gordo and Xavier labs for critically reading earlier versions of this manuscript. This work was funded by the the Marie

Sklodowska-Curie Actions (MSCA) with the fellowship 746690-ResistEpist-H2020-MSCA-IF-2016/H2020-MSCA-IF-2016, to R.B., and partially supported by ONEIDA project (LISBOA-01-0145-FEDER-016417) co-funded by FEEI - "Fundos Europeus Estruturais e de Investimento" from "Programa Operacional Regional Lisboa 2020", and by national funds from "Fundação para a Ciência e a Tecnologia" (FCT), to I.G. R.B. was also supported by the FCT with the fellowship SFRH/BDP/109517/2015. The authors declare no conflicts of interest.

Author contributions

R.B: conceptualization, formal analysis, funding acquisition, investigation, methodology, visualization, writing – original draft. I.G: conceptualization, formal analysis, funding acquisition, methodology, project administration, resources, supervision, writing – review & editing.

Declaration of interests

The authors declare no competing interests.

Data availability

All the strains used (Data S1) are available via Material Transfer Agreement (MTA). The raw data of the experiments shown in all figures and the table are available as Additional Information in

Data S2. The images analyzed to obtain the data shown in Table 1, and those used in Figures S1 and S2 are available in the public data repository Zenodo (DOI: 10.5281/zenodo.3381746).

Materials and methods

Bacterial strains, media and growth conditions

All the strains used in this study (Data S1) derive from strains RB266, RB323 or RB324, which are derivatives of *E. coli* K12 MG1655 (Blattner *et al.*, 1997). Fluorescently labeled strains harbor a copy of either YFP or CFP under the control of the lac-regulated promoter P_{LacO-1} inserted either in the *yzgL* pseudogene locus or in the *galK* gene, a deletion comprising the entire *lac* operon (to make constitutive the expression of the fluorescent proteins), and the SOS reporter construction P_{sulA}-*mCherry* inserted in the *ysaCD* pseudogene locus. The SOS reporter fusion was constructed by replacing a *tetA-sacB* selectable/counterselectable marker (Li, Thomason, Sawitzke, Costantino, & Court, 2013) located upstream from a *mCherry-FRT-aph-FRT* cassette previously inserted in the *ysaCD* locus by the regulatory regions (150bp upstream from the translation initiation site) of the SOS-regulated gene *sulA*. Resistant mutants additionally carry different chromosomal alleles conferring antibiotic resistance/s. The fluorescent constructions were generated by Lambda-Red recombineering (Murphy, Campellone, & Poteete, 2000, Yu *et al.*, 2000, Datsenko & Wanner, 2000), followed by transference to a clean background by P1 transduction (Lennox, 1955), and subsequent transduction of the resistance alleles. The clean deletion of *rnhA* was constructed by markerless recombineering using

a *tetR-*P_{tet}*-ccdB-cat* selection/counterselection cassette as described in Figueroa-Bossi & Bossi (Figueroa-Bossi & Bossi, 2015), and subsequent transfer of the markerless deletion to a clean background by P1 transduction, using as recipient an isogenic strain carrying a deletion of the nearby gene *proB*, which causes proline auxotrophy, and selecting for growth in minimal medium. The presence of each construction/mutation was assessed by PCR-mediated amplification of the corresponding region and Sanger sequencing. The Gam-GFP construction (Shee *et al.*, 2013) was generously contributed by Professor Susan M. Rosenberg. The chromosomal construction comprising a copy of the *rnhA* gene under the control of a promoter inducible by arabinose (Stockum *et al.*, 2012) was kindly donated by Dr. Christian J. Rudolph. Derivatives of these strains carrying the P_{sulA}*-mCherry* and different resistance mutations were constructed by P1 transduction. The plasmid pRB-5 (carrying the *rnhA* gene under the control of a promoter inducible by anhydrotetracycline) was constructed by PCR amplification of the vector pZS*11 (Subramaniam, Pan, & Cluzel, 2013) and the construction *tetR-*$P_{LTetO-1}$*-rnhA* from strain RB1207, subsequent restriction with AatII and HindIII enzymes, ligation and electroporation. The construction *tetR-*$P_{LTetO-1}$*-rnhA* in strain RB1207 was made by Lambda-Red recombineering (Murphy, Campellone, & Poteete, 2000, Yu *et al.*, 2000, Datsenko & Wanner, 2000), and selection/counterselection (Li *et al.*, 2013), over a previous $P_{LtetO-1}$*-sfGFP* construction (Balbontín, Vlamakis, & Kolter, 2014). Cultures were grown in either Lysogeny Broth (LB, Miller formulation) (Bertani, 1951) or M9 broth supplemented with 0.4% glucose (*Maniatis et al. Molecular cloning: A laboratory manual (CSHL Press)*), in round-bottom 96-well plates incubated at 37°C with shaking (700 r.p.m.) in a Grant-bio PHMP-4 benchtop incubator, unless indicated otherwise. Solid medium was LB containing 1.5% agar, supplemented when necessary with antibiotics at the following concentrations:

rifampicin (100 µg/ml), streptomycin (100 µg/ml), ampicillin (100 µg/ml), erythromycin (150 µg/ml), kanamycin (100 µg/ml), chloramphenicol (25 µg/ml).

Competitive fitness/SOS induction assays

The relative fitness (selection coefficient per generation) of each YFP-tagged resistant strain carrying the SOS reporter was measured by competitive growth against an isogenic sensitive strain *E. coli* K12 MG1655 constitutively expressing CFP and also carrying the SOS reporter. The formula used to calculate the selection coefficient was $s=\left[\ln\left(NRf/NSf\right)-\ln\left(NRi/NSi\right)\right]\ln\left(NSf/NSi\right)$, being ***NRi*** and ***NRf*** the initial and final number of resistant bacteria, and ***NSi*** and ***NSf*** the initial and final number of sensitive bacteria. The competitor strains were first streaked out of their respective frozen vials, then individual colonies were inoculated separately in medium without antibiotics and incubated overnight (approximately 16h); the next morning, the number of cells in each culture was measured by Flow Cytometry, and 10 µl of 1:1 mixtures of YFP and CFP bacteria were added to 140 µl of medium, at an initial number of approximately 10^6 cells. The initial and final frequencies of the strains were obtained by counting their cell numbers in the Flow Cytometer. Generation time was estimated from the doubling time of the reference strain (approximately five generations at 4h, and approximately eight generations at 24h), and the selection coefficient was determined as described above for each independent competition. The proportion of SOS-induced bacteria was quantified as the number of either YFP-tagged or CFP-labeled bacteria showing red fluorescence (from the P_{sulA}-*mCherry* SOS

reporter fusion) above a threshold determined by the fluorescence levels of the control strains *lexA (ind-)* (constitutive repression of the SOS response) and *ΔlexA* (constitutive activation of the SOS response) *(Lin & Little, 1988)*. The data represented is the induction level of each mutant normalized with respect to the induction levels of the sensitive it is competing against. In the competitions including the RNase HI inhibitor 2-[[[3-Bromo-5-(2-furanyl)-7-(trifluoromethyl)pyrazolo[1,5-a]pyrimidin-2-yl]carbonyl]amino]-4,5,6,7-tetrahydro-benzo[b]thiophene-3-carboxylic acid ethyl ester (RHI001), the medium was supplemented with 500 µM of RHI001 (Glixx Laboratories Inc., catalog number GLXC-03982).

Flow Cytometry

A BD LSR Fortessa™ SORP flow cytometer was used to quantify bacteria, using a 96-well plate High-Throughput Sampler (HTS) and SPHERO fluorescent spheres (AccuCount 2.0 µm blank particles), in order to accurately measure volumes. Bacterial numbers were calculated based on the counts of fluorescently labeled bacteria with respect the known number of beads added to a given volume. The instrument was equipped with a 488 nm laser used for scatter parameters and YFP detection, a 442 nm laser for CFP detection and a 561 nm laser for mCherry detection. Relative to optical configuration, CFP, YPF and mCherry were measured using bandpass filters in the range of 470/20 nm, 540/30 nm and 630/75nm, respectively. The analyzer is also equipped with a forward scatter (FSC) detector in a photomultiplier tube (PMT) to detect bacteria. The samples were acquired using FACSDiVa (version 6.2) software, and analyzed using FlowJo (version X 10.0.7r2). All Flow

Cytometry experiments were performed at the Flow Cytometry Facility of Instituto Gulbenkian de Ciência, Oeiras, Portugal.

Selection for Erm^R bacteria

Fifteen independent colonies of sensitive bacteria were separately inoculated in LB in a 96-well plate, incubated at at 37°C with shaking (700 r.p.m) for 7 hours, and 0.1ml of either independent culture was plated onto a LB agar plate supplemented with 150 µg/ml erythromycin, and incubated at 37°C for 5 days (Erm^R strains grow in the presence of erythromycin, albeit slowly). Colonies able to grow in these plates were streaked onto plates supplemented with 150 µg/ml erythromycin, in order to further assess their *bona fide* resistance, and the *rplD*, and *rplV* genes of the resistant clones were amplified by PCR and analyzed by Sanger sequencing.

Microscopy

Early exponential cultures were diluted into pre-warmed medium containing the inducer of the Gam-GFP construction (anhydrotetracycline, 25ng/ml) and incubated at 37°C with shaking (240 r.p.m.) for 3h, prior to imaging. Bacterial solutions were then placed onto 1% agarose (in 1X PBS) pads mounted in adhesive frames between the microscope slide and a coverglass. Images were acquired on an Applied Precision DeltavisionCORE system, mounted on an Olympus IX71 inverted microscope,

coupled to a Cascade II 1024x1024 EM-CCD camera, using an Olympus 100x 1.4NA Uplan SAPO Oil immersion objective, where GFP and mCherry were imaged with FITC (Ex: 475/28, EM: 528/38) and TRITC (Ex: 542/28, Em: 617/73) fluorescence filtersets, respectively, and DIC optics. Images were deconvoluted with Applied Precision's softWorx software, and prepared for presentation (cropping smaller fields to facilitate visualization, and false-coloring green and red fluorescent signals) using Fiji/ImageJ.

Long-term propagations of polymorphic populations

The CFP-tagged sensitive (either WT or *ΔrnhA*) and the five YFP-labeled resistant bacterial (either RpsL^{K43N}, RpsL^{K43T}, RpoB^{H526L}, RpoB^{H526Y}, and RpoB^{S531F} or *ΔrnhA* RpsL^{K43N}, *ΔrnhA* RpsL^{K43T}, *ΔrnhA* RpoB^{H526L}, *ΔrnhA* RpoB^{H526Y}, and *ΔrnhA* RpoB^{S531F}) were streaked individually onto LB agar plates and incubated overnight at 37°C. The next day, three independent colonies from each strain were inoculated separately in LB broth (150 µl per well) in a 96-well plate and incubated overnight at 37°C with shaking (700 r.p.m). The next day, bacteria were quantified by Flow Cytometry, and 10 µl of 1:1:1:1:1:1 mixtures of the sensitive and either resistant bacteria were added to 140 µl of medium, at a initial number of approximately 10^6 cells. The initial frequencies of the fluorescent strains were confirmed by Flow Cytometry. Every 24h, during 15 days, 10 µl of bacteria culture was diluted by a factor of 10^{-2}, then transferred to 140 µl fresh LB and allowed to grow for additional 24h, reaching approximately 10^9 cells/ml. In parallel, cell numbers were counted using the Flow Cytometer, in order

417 to measure the frequency of each strain in the mixed population during the experiment, by collecting a
418 sample (10 µl) from the spent culture each day.
419
420 Growth curves
421
422 YFP-tagged sensitive and RpsL^{K43N} RpoB^{H526Y} strains were streaked individually onto LB agar
423 plates and incubated overnight at 37°C. The next day, three independent colonies from each strain were
424 inoculated separately in LB broth (150 µl per well) in a 96-well plate and incubated overnight at 37°C
425 with shaking (700 r.p.m). The next day, bacteria were quantified by Flow Cytometry, and
426 approximately $5x10^5$ bacteria were inoculated in 100-well plates containing LB broth supplemented
427 with either 0.5% DMSO (the solvent of RHI001) or 50 µM RHI001 (150 µl per well), and incubated at
428 37ºC with continuous shaking (medium amplitude, duration 5s, 10s interval, and stopping 5s before
429 each measurement) in a Bioscreen C (Oy Growth Curves Ab Ltd.) benchtop plate reader, measuring
430 OD_{600} every 30 minutes during 12h.
431
432 Statistical analyses
433
434 All analyses were conducted using Libreoffice Calc version 5.4.1.2 (www.libreoffice.org)
435 software, R version 3.4.4 (www.r-project.org) software via RStudio version 1.1.442 interface
436 (www.rstudio.com) and GraphPad Prism version 7.04 (www.graphpad.com). For each set of
437 competitions (n≥3), two-tailed unpaired Student's *t*-tests were used. For testing the association between

the fitness cost and the level of SOS induction, a linear regression of the s with the logarithm of the fold change in SOS induction of each resistant clone (with respect to the sensitive bacteria it is competing against in the same well), was used.

Figures

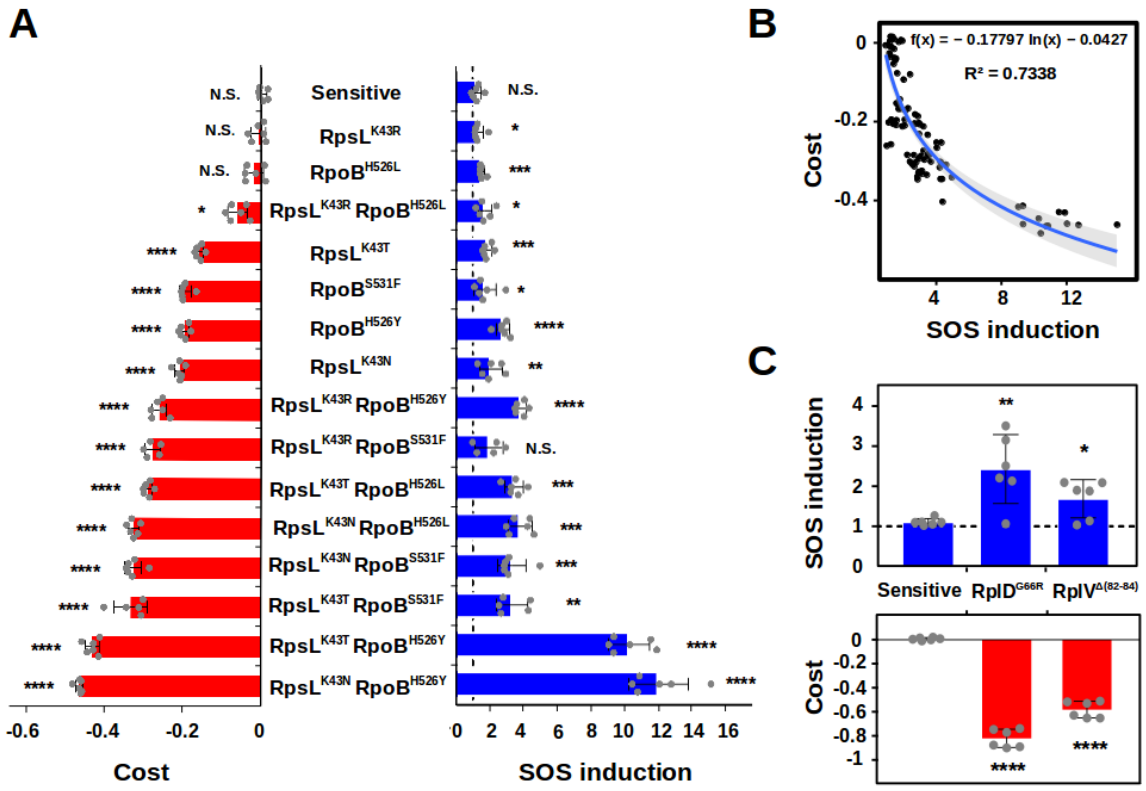

Figure 1. DNA breaks explain variation in the fitness cost of resistance. A. Fitness cost (red bars) and SOS induction (blue bars) of sensitive bacteria and Str^R and Rif^R mutants in LB broth at 4 hours. The strains are ordered from lower to higher fitness cost (top to bottom). The dashed line indicates no SOS induction. Error bars represent mean ± standard deviation of independent biological replicates (n≥5). N.S. non-significant; *P < 0.05; **P < 0.01; ***P < 0.001; ****P < 0.0001 (two-tailed Student's t test). **B.** Correlation between the fitness cost (y axis) and the SOS induction (x axis) representing all the data points from A. The blue line represents the logarithmic regression line, and the grey area represents the 95% confidence interval. **C.** SOS induction (blue bars) and fitness cost (red bars) of sensitive bacteria and Erm^R mutants in LB broth at 4 hours. The dashed line indicates no SOS induction. Error bars represent mean ± standard deviation of independent biological replicates (n=6). N.S. non-significant; *P < 0.05; **P < 0.01; ***P < 0.001; ****P < 0.0001 (two-tailed Student's t test).

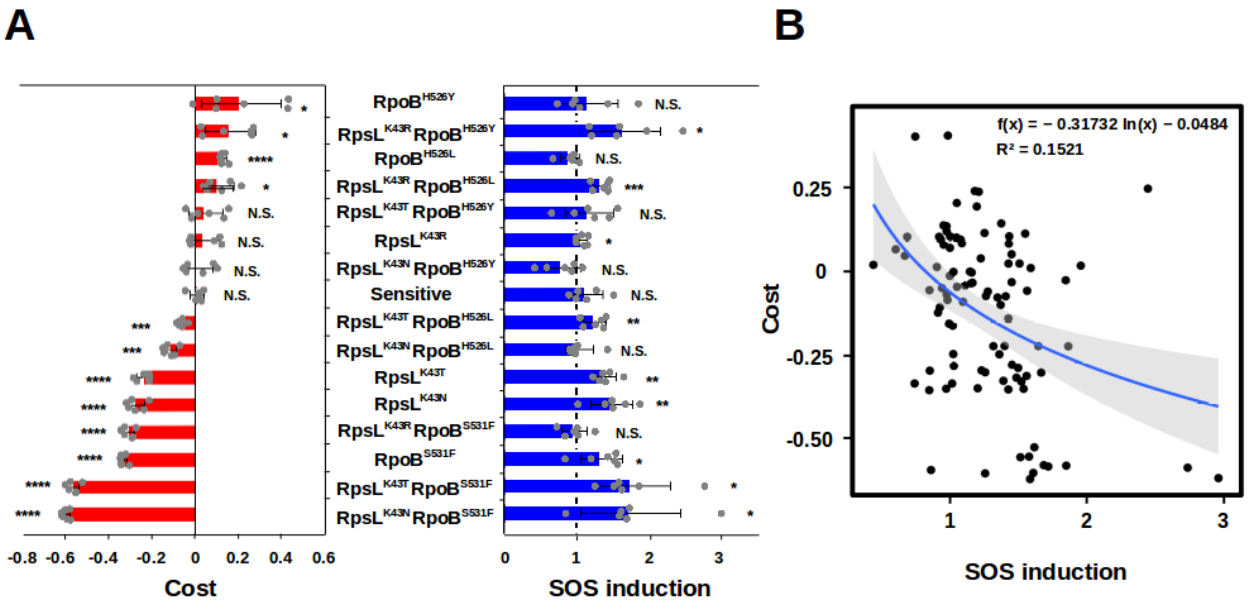

Figure 2. DNA breaks are reduced in minimal medium. **A.** Fitness cost (red bars), and SOS induction (blue bars) of sensitive bacteria and Str^R and/or Rif^R mutants in minimal medium at 8 hours. The strains are ordered from lower to higher cost (top to bottom). The dashed line indicates no SOS induction. Error bars represent mean ± standard deviation of independent biological replicates (n=6). N.S. non-significant; **P* < 0.05; ***P* < 0.01; ****P* < 0.001; *****P* < 0.0001 (two-tailed Student's *t* test). **B.** Correlation between the fitness cost (y axis) and the SOS induction (x axis) representing all the data points from panel A. The blue line represents the logarithmic regression line, and the grey area represents the 95% confidence interval.

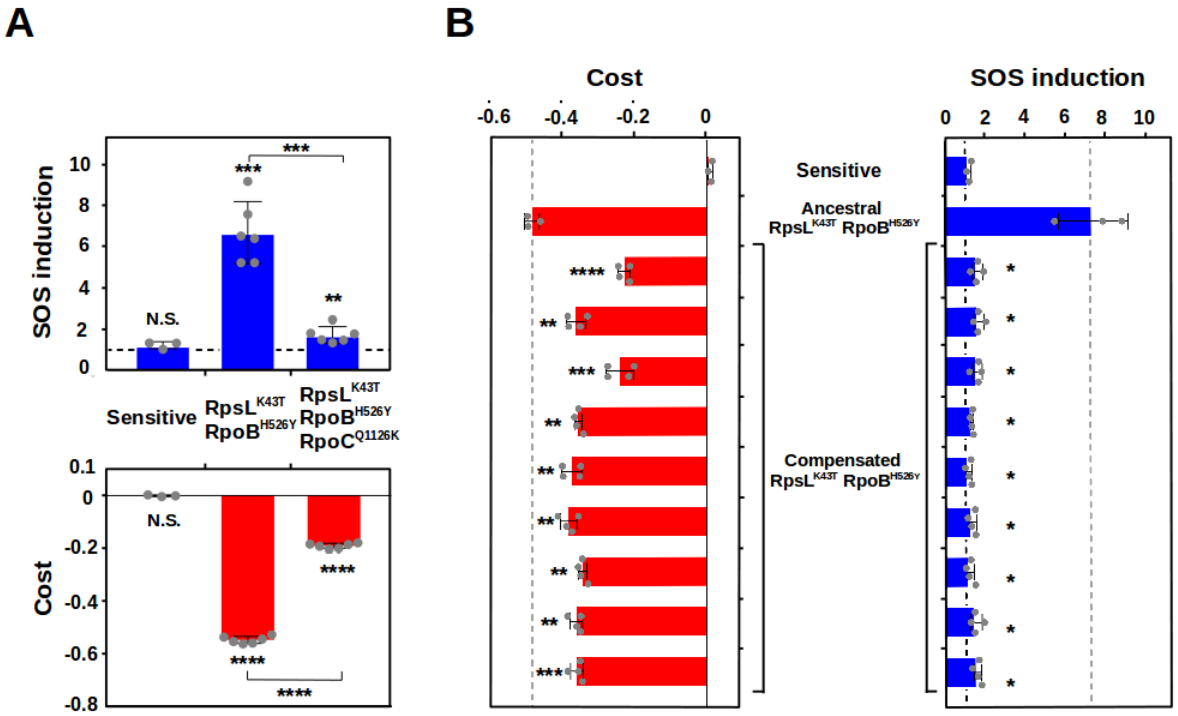

460 **Figure 3. Compensatory evolution cause reduction of DNA breaks. A.** SOS induction (blue bars) and fitness
461 cost (red bars), of sensitive (left) double resistant (center) and double resistant carrying a compensatory mutation
462 (right) bacteria in LB broth at 4 hours. The dashed line indicates no SOS induction. Error bars represent mean ±
463 standard deviation of independent biological replicates (n≥3). N.S. non-significant; *$P < 0.05$; **$P < 0.01$; ***P
464 < 0.001; ****$P < 0.0001$ (two-tailed Student's *t* test). **B.** Fitness cost (red bars), and SOS induction (blue bars)
465 of sensitive, ancestral RpsL^{K43T} RpoB^{H526Y} and nine compensated RpsL^{K43T} RpoB^{H526Y} clones in LB broth at 4
466 hours. The black dashed line indicates no SOS induction. The grey dashed lines mark the cost/SOS of the
467 ancestral double mutant. Error bars represent mean ± standard deviation of independent biological replicates
468 (n≥3). N.S. non-significant; *$P < 0.05$; **$P < 0.01$; ***$P < 0.001$; ****$P < 0.0001$ (two-tailed Student's *t* test).

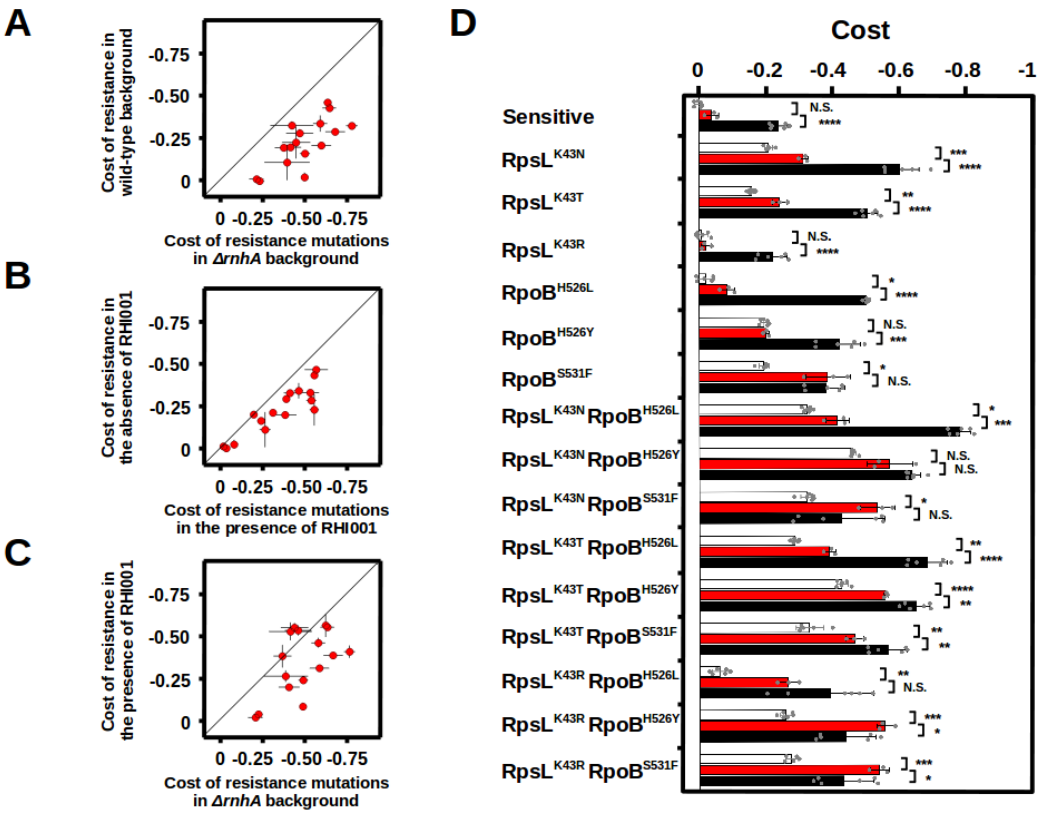

Figure 4. RNAse HI strongly influences the fitness of resistant bacteria. A. Correlation between the fitness cost of resistance mutations in wild-type (y axis) or *ΔrnhA* backgrounds (x axis). **B.** Correlation between the fitness cost of resistance mutations in the absence of the RNase HI inhibitor (y axis) or in its presence (x axis). **C.** Correlation between the fitness cost of resistance mutations in the presence of the RHI001 (y axis) or in the *ΔrnhA* background (x axis). The values corresponding to the wild-type background in panel A and to absence of RHI001 in panel B are those shown in Figure 1A. Error bars represent mean ± standard deviation of independent biological replicates (n≥3). The black line in panels A-C represents the linear regression if the costs were identical **D.** Fitness cost of sensitive bacteria and Str^R and/or Rif^R mutants in the presence of the RNase HI inhibitor RHI001 (red bars). For comparison, the corresponding values in the absence of the inhibitor (data from the experiments shown in Figure 1A) or in a *ΔrnhA* background (data from the experiments shown in panel A and Figure S3A) are represented as white and black bars, respectively. Error bars represent mean ± standard deviation of independent biological replicates (n=3). N.S. non-significant; *$P < 0.05$; **$P < 0.01$; ***$P < 0.001$; ****$P < 0.0001$ (two-tailed Student's *t* test). See also Figures S3, S4 and S5.

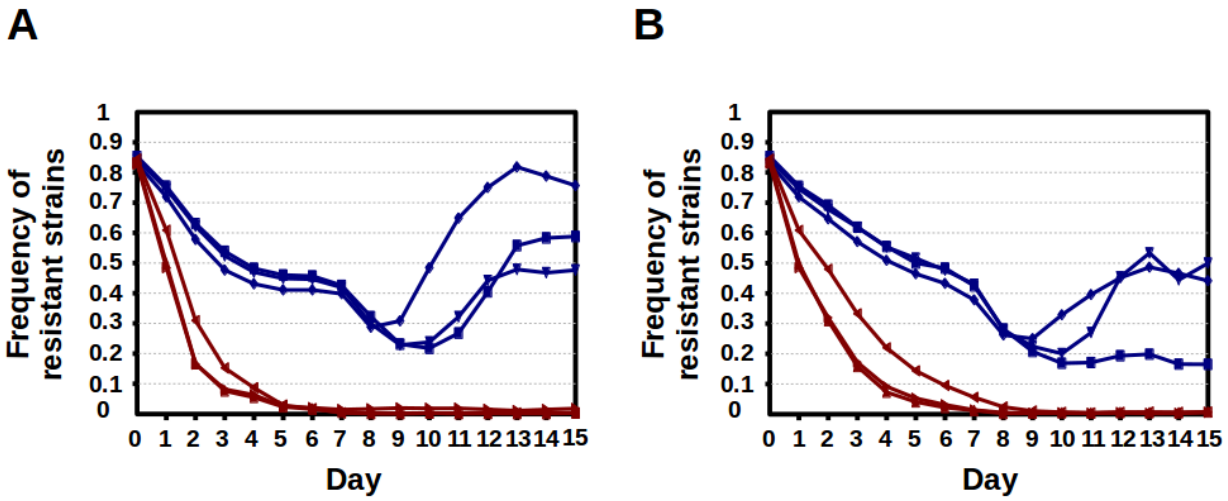

Figure 5. Lack of RNase HI favors outcompetition of resistant mutants by sensitive bacteria. Frequency of single resistant mutants during three independent long-term competitions against sensitive bacteria either in a genetic background including RNase HI (blue lines) or in a *ΔrnhA* background (red lines), imposing either a strong (1:1500 dilutions) (**A**) or a mild (1:50 dilutions) (**B**) bottlenecks.

Tables

Table 1. Percentage of cells showing DNA breaks (Gam-GFP foci) in sensitive and resistant bacteria either in wild-type or *ΔrnhA* backgrounds. Except in the *Δdam* positive control (in which over 100 cells sufficed to provide an illustrative example), at least 1000 cells per group were analyzed. See also Figures S1 and S2.

***Δdam* (positive control)**	**21.28%**
Sensitive	**0.72%**
rpsL (K43N)	**0.73%**
rpoB (H526Y)	**0.96%**
rpsL (K43N) rpoB (H526Y)	**10.71%**
***ΔrnhA* (sensitive)**	**9.27%**
ΔrnhA rpsL (K43N)	**33.92%**
ΔrnhA rpoB (H526Y)	**10.02%**
ΔrnhA rpsL (K43N) rpoB (H526Y)	**49.90%**

Supplemental Figures

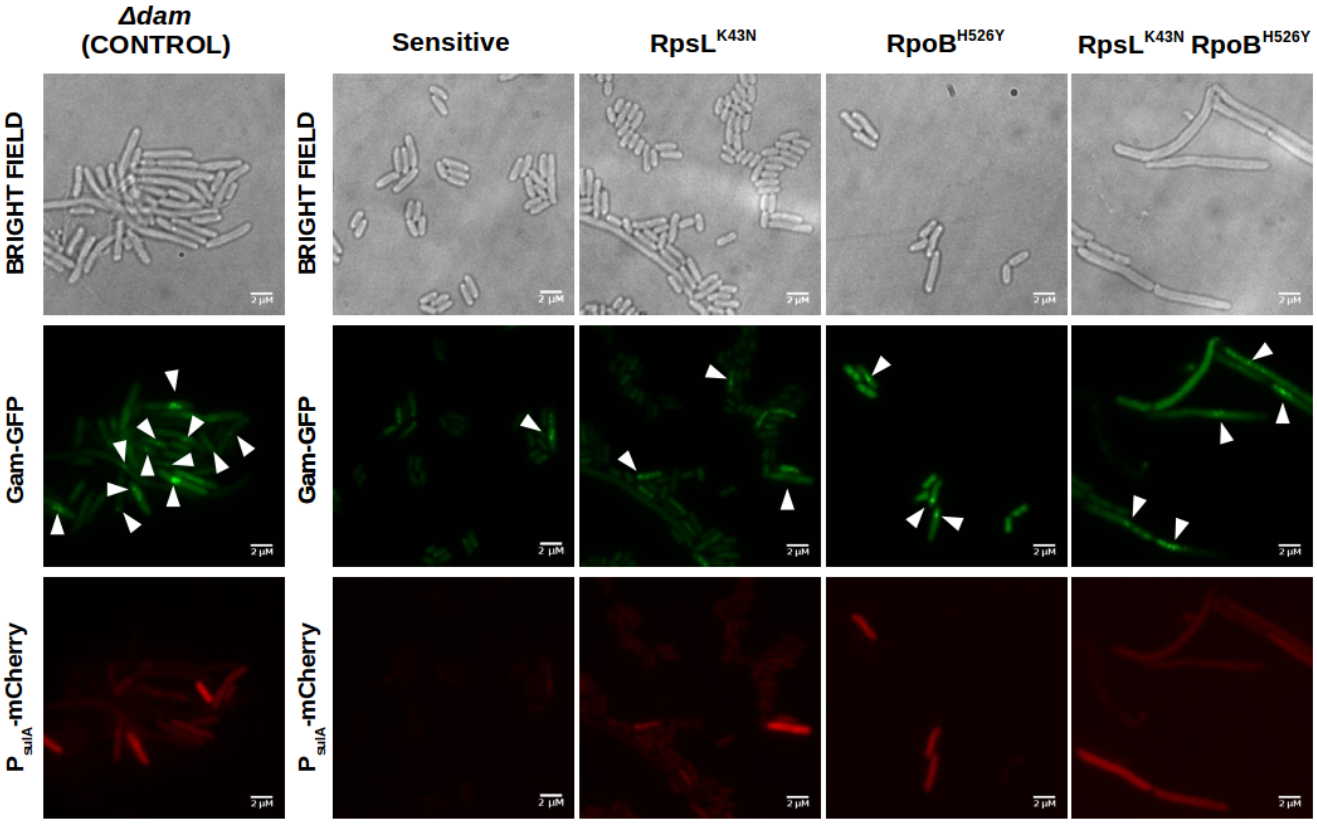

Figure S1. Visualization of DNA breaks and SOS induction of sensitive, single and double resistant strains by epifluorescence microscopy. Bacterial cells show a disperse faint green fluorescence distributed along the cytoplasm, unless DNA breaks are present; upon generation of DNA breaks, the disperse fluorescence concentrates in bright fluorescent foci (central panels, false-colored in green). Red fluorescence (bottom panels, false-colored in red) is absent until the SOS response is induced due to the presence of DNA breaks. Cell elongation (top panels) is a well-known phenotype derived from the inhibition of cell division by SOS-regulated proteins.

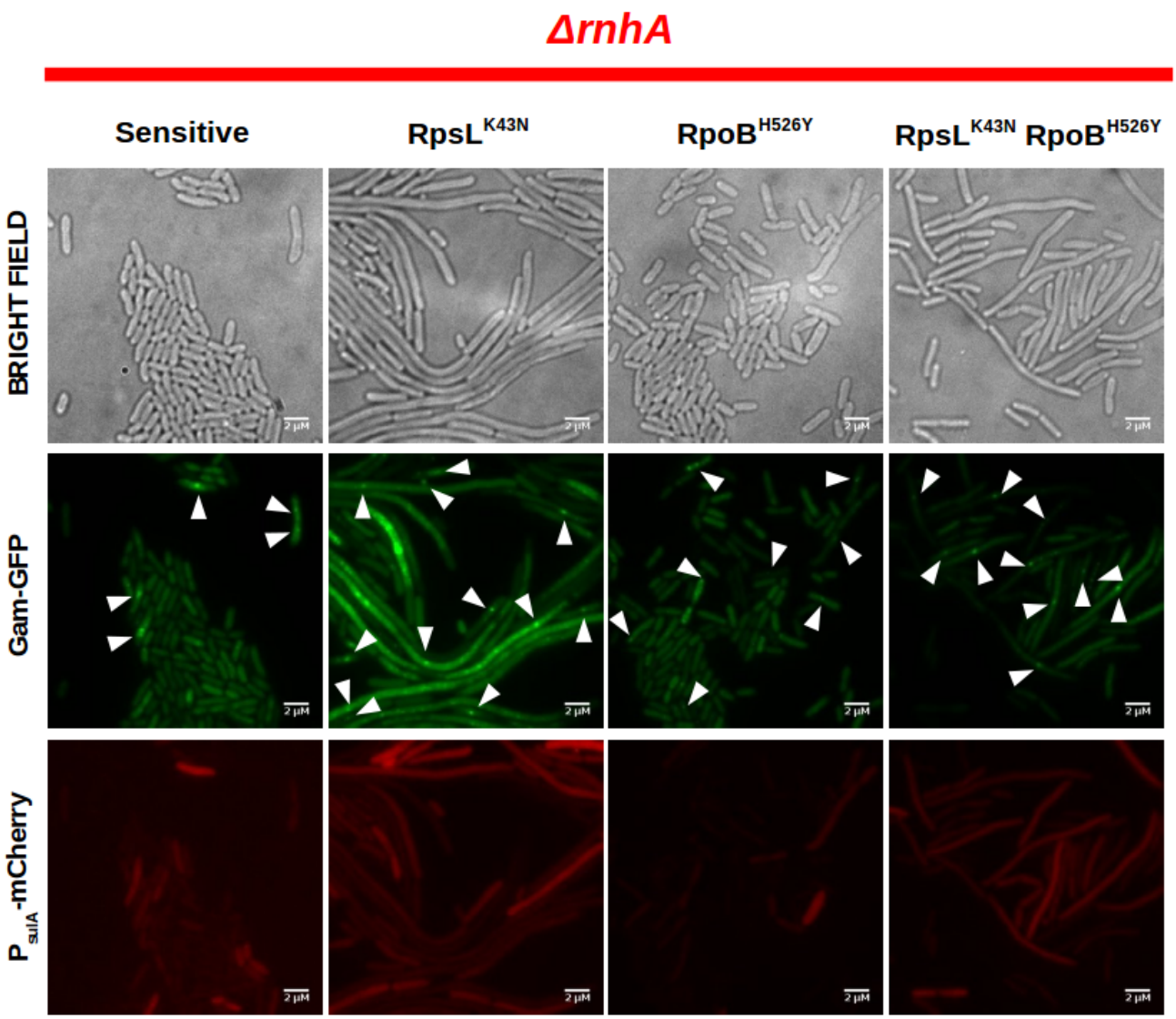

Figure S2. Visualization of DNA breaks and SOS induction of sensitive, single and double resistant strains in *ΔrnhA* background by epifluorescence microscopy. Bacterial cells show a disperse faint green fluorescence distributed along the cytoplasm, unless DNA breaks are present; upon generation of DNA breaks, the disperse fluorescence concentrates in bright fluorescent foci (central panels, false-colored in green). Red fluorescence (bottom panels, false-colored in red) is absent until the SOS response is induced due to the presence of DNA breaks. Cell elongation (top panels) is a well known phenotype derived from the inhibition of cell division by SOS-regulated proteins.

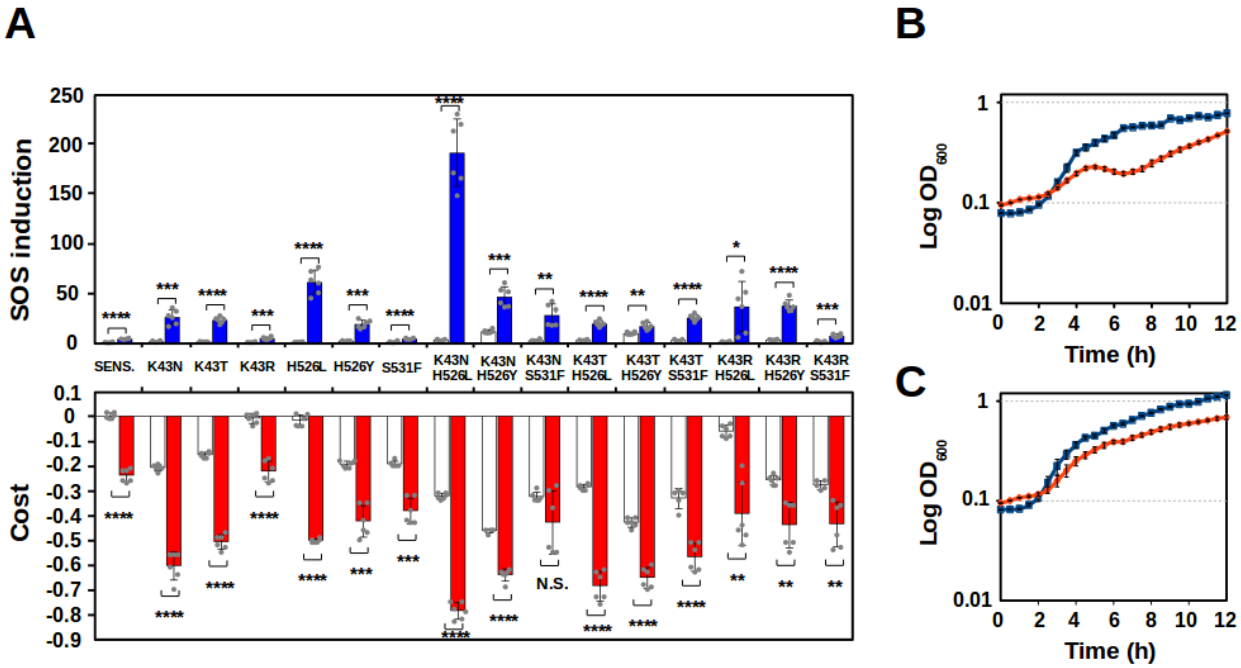

509 **Figure S3. Depletion of RNase HI increases fitness cost and SOS induction. A.** SOS induction (blue bars)
510 and fitness cost (red bars), of sensitive bacteria and Str^R and/or Rif^R mutants (labels represent the corresponding
511 allele/s) in a *ΔrnhA* background. The white bars represent the corresponding values in bacteria with an intact
512 *rnhA* gene (data from the experiments shown in Figure 1A), for comparison. Error bars represent mean ±
513 standard deviation of independent biological replicates (n=6). N.S. non-significant; **P* < 0.05; ***P* < 0.01; ****P*
514 < 0.001; *****P* < 0.0001 (two-tailed Student's *t* test). **B.** Growth curves of $RpsL^{K43N}$ $RpoB^{H526Y}$ double mutant in
515 the presence of either DMSO (blue lines) or RHI001 (orange lines). Points and error bars represent mean ±
516 standard deviation of independent biological replicates (n=3). **C.** Growth curves of sensitive bacteria in the
517 presence of either DMSO (blue lines) or RHI001 (orange lines). Points and error bars represent mean ± standard
518 deviation of independent biological replicates (n=3).

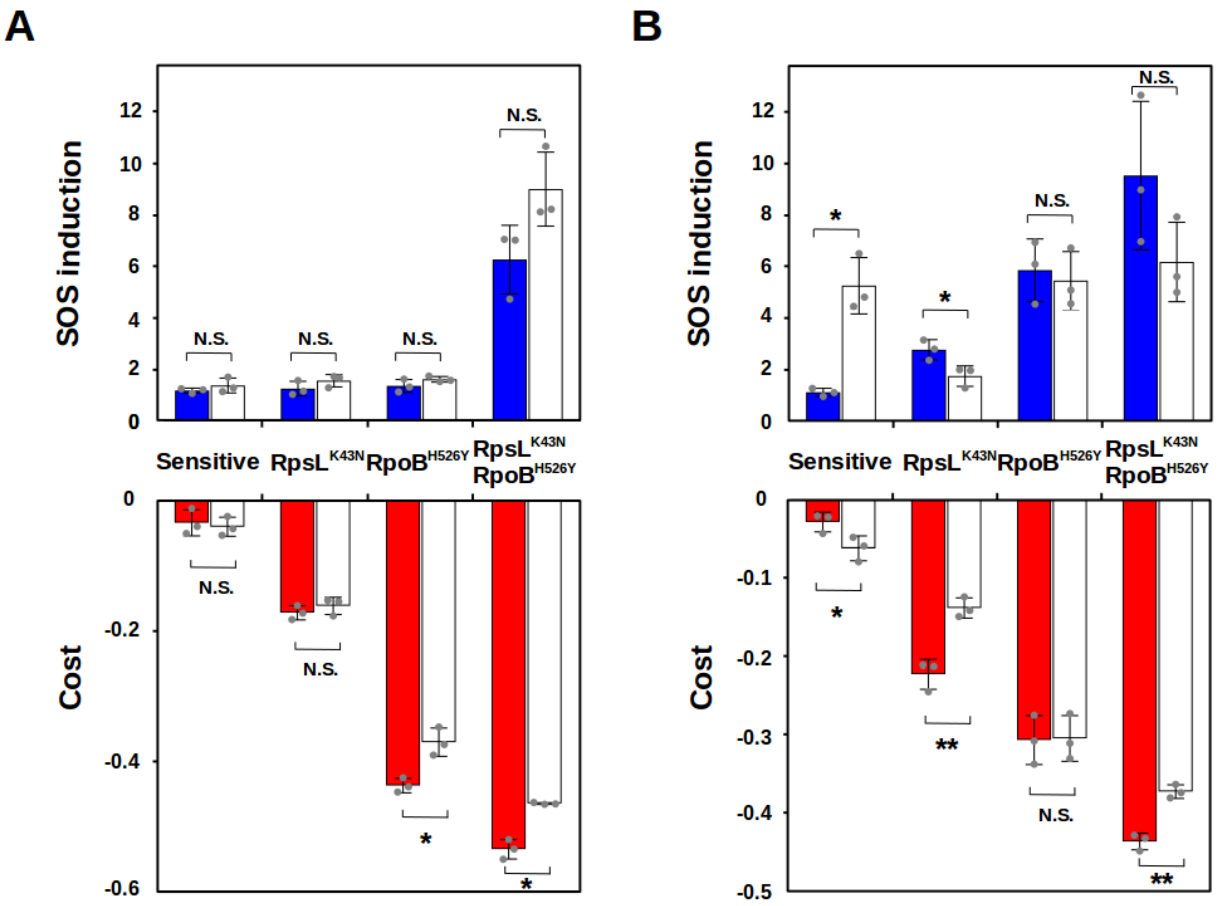

519 **Figure S4. Mild overproduction of RNase HI can ameliorate both cost and SOS induction.** SOS induction
520 (top) and fitness cost (bottom), of sensitive bacteria (left), two single resistant mutants (center) and the double
521 mutant combining these two alleles (right) in LB broth at 4h (**A**) or 24h (**B**) in a background harboring an
522 additional chromosomal copy of the gene encoding the RNase HI (*rnhA*) under the control of the arabinose
523 promoter, either in the absence (red bars) or the presence (white bars) of arabinose. Error bars represent mean ±
524 standard deviation of independent biological replicates (n=3). N.S. non-significant; **P* < 0.05; ***P* < 0.01; ****P*
525 < 0.001; *****P* < 0.0001 (two-tailed Student's *t* test).

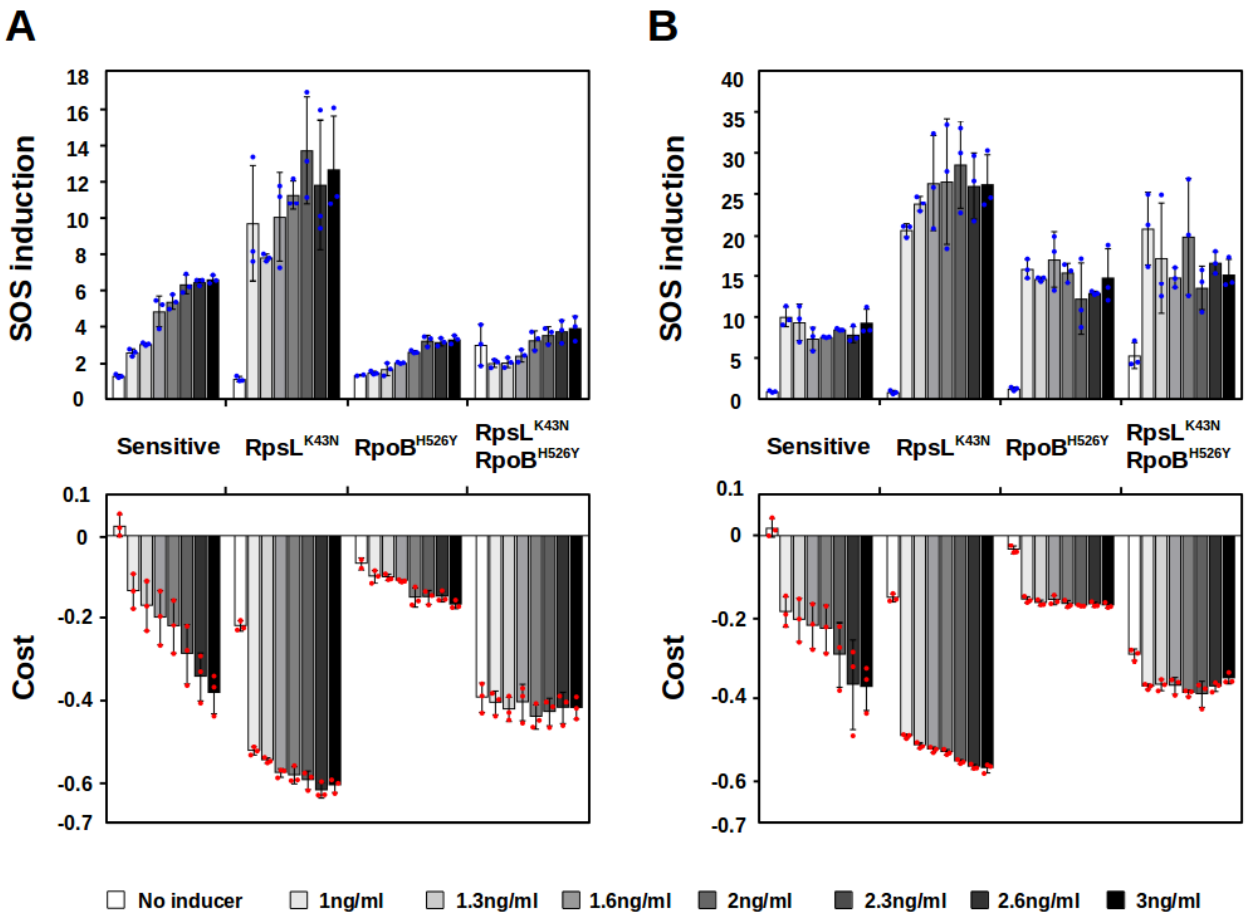

Figure S5. Strong overproduction of RNase HI increases cost and SOS induction in all the backgrounds. SOS induction (top) and fitness cost (bottom), of sensitive bacteria (left), two single resistant mutants (center) and the double mutant combining these two alleles (right) in LB broth at 4h (**A**) or 24h (**B**) in a background harboring a plasmid carrying a copy of the RNase HI gene (*rnhA*) under the control of a promoter inducible by anhydrotetracycline, either in the absence (white bars) or the presence of different concentrations of the inducer (greyscale, from light grey to black bars). Error bars represent mean ± standard deviation of independent biological replicates (n≥2). N.S. non-significant; **P* < 0.05; ***P* < 0.01; ****P* < 0.001; *****P* < 0.0001 (two-tailed Student's *t* test).

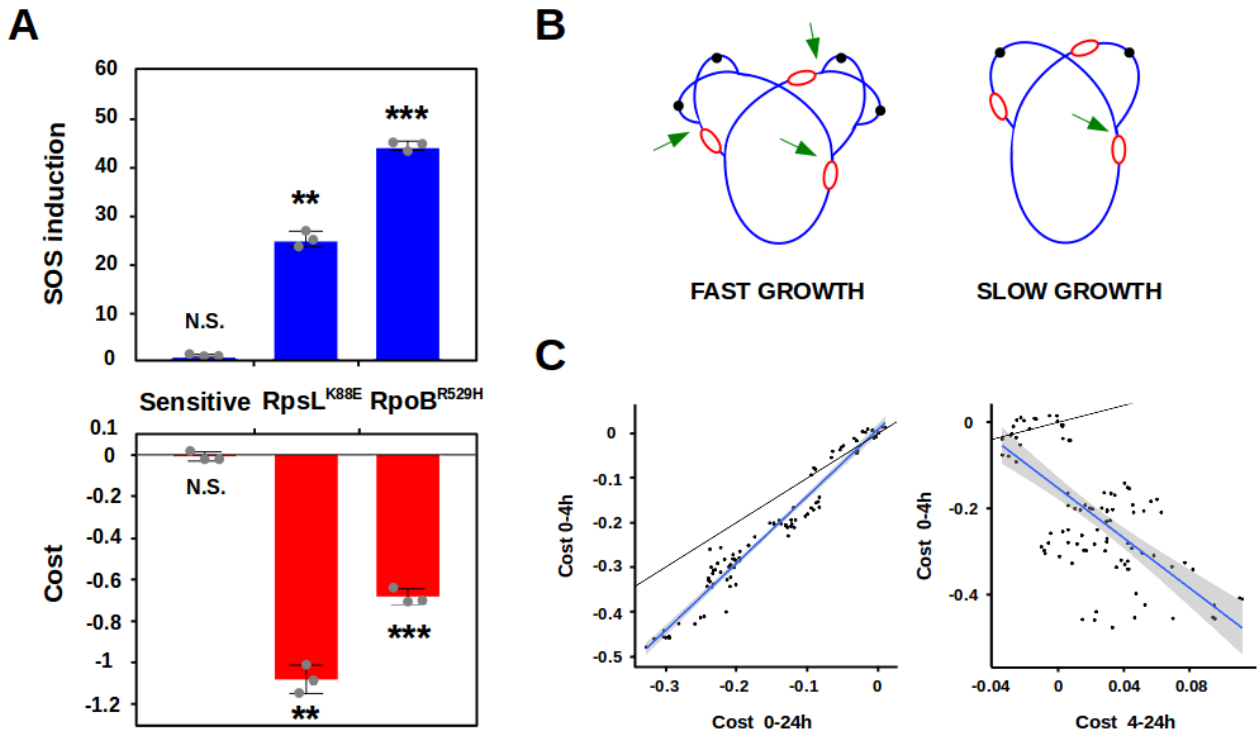

534 **Figure S6. A. Costly single mutants show increased SOS induction.** SOS induction (blue bars) and fitness
535 cost (red bars), of sensitive bacteria (left) and two costly single resistant mutants (center and right). Error bars
536 represent mean ± standard deviation of independent biological replicates (n=3). N.S. non-significant; *$P < 0.05$;
537 **$P < 0.01$; ***$P < 0.001$; ****$P < 0.0001$ (two-tailed Student's t test). B. Schematic representation of multi-
538 fork DNA replication of *E. coli* during fast (left) or slow (right) growth. Black dots represent the origin of
539 replication, and red lines represent transcription forks; green arrows mark regions of potential conflicts between
540 replication and transcription forks. **C. Costs are expressed during fast growth**. Data from the experiments
541 shown in Figure 1A. Left panel: correlation between the fitness cost between time 0 and 4h (y axis) and between
542 time 0 and 24h (y axis), in LB broth. Right panel: correlation between the fitness cost between time 0 and 4h (y
543 axis) and between time 4h and 24h (y axis), in LB broth. Black lines represent the linear regressions if the costs
544 were identical. Blue lines represent the regression lines, and the grey areas represent the 95% confidence
545 intervals.

546 **References**

547

Almeida Da Silva, P. E. A., & Palomino, J. C. (2011). Molecular basis and mechanisms of drug resistance in Mycobacterium tuberculosis: Classical and new drugs. *The Journal of Antimicrobial Chemotherapy*, *66*(7), 1417–1430. https://doi.org/10.1093/jac/dkr173

Andersson, D. I., & Levin, B. R. (1999). The biological cost of antibiotic resistance. *Current Opinion in Microbiology*, *2*(5), 489–493.

Andersson, Dan I., & Hughes, D. (2010). Antibiotic resistance and its cost: Is it possible to reverse resistance? *Nature Reviews. Microbiology*, *8*(4), 260–271. https://doi.org/10.1038/nrmicro2319

Applebee, M. K., Herrgård, M. J., & Palsson, B. Ø. (2008). Impact of individual mutations on increased fitness in adaptively evolved strains of Escherichia coli. *Journal of Bacteriology*, *190*(14), 5087–5094. https://doi.org/10.1128/JB.01976-07

Balbontín, R., Vlamakis, H., & Kolter, R. (2014). Mutualistic interaction between Salmonella enterica and Aspergillus niger and its effects on Zea mays colonization. *Microbial Biotechnology*, *7*(6), 589–600. https://doi.org/10.1111/1751-7915.12182

Bertani, G. (1951). Studies on lysogenesis. I. The mode of phage liberation by lysogenic Escherichia coli. *Journal of Bacteriology*, *62*(3), 293–300.

Birge, E. A., & Kurland, C. G. (1969). Altered ribosomal protein in streptomycin-dependent Escherichia coli. *Science (New York, N.Y.)*, *166*(3910), 1282–1284. https://doi.org/10.1126/science.166.3910.1282

Blattner, F. R., Plunkett, G., Bloch, C. A., Perna, N. T., Burland, V., Riley, M., … Shao, Y. (1997). The complete genome sequence of Escherichia coli K-12. *Science (New York, N.Y.)*, *277*(5331), 1453–1462. https://doi.org/10.1126/science.277.5331.1453

Bohman, K., Ruusala, T., Jelenc, P. C., & Kurland, C. G. (1984). Kinetic impairment of restrictive streptomycin-resistant ribosomes. *Molecular & General Genetics: MGG*, *198*(2), 90–99. https://doi.org/10.1007/bf00328706

Broccoli, S., Rallu, F., Sanscartier, P., Cerritelli, S. M., Crouch, R. J., & Drolet, M. (2004). Effects of RNA polymerase modifications on transcription-induced negative supercoiling and associated R-loop formation. *Molecular Microbiology*, *52*(6), 1769–1779. https://doi.org/10.1111/j.1365-2958.2004.04092.x

Burmann, B. M., Schweimer, K., Luo, X., Wahl, M. C., Stitt, B. L., Gottesman, M. E., & Rösch, P. (2010). A NusE:NusG complex links transcription and translation. *Science (New York, N.Y.)*, *328*(5977), 501–504. https://doi.org/10.1126/science.1184953

Chittum, H. S., & Champney, W. S. (1994). Ribosomal protein gene sequence changes in erythromycin-resistant mutants of Escherichia coli. *Journal of Bacteriology*, *176*(20), 6192–6198. https://doi.org/10.1128/jb.176.20.6192-6198.1994

Das, A., Merril, C., & Adhya, S. (1978). Interaction of RNA polymerase and rho in transcription termination: Coupled ATPase. *Proceedings of the National Academy of Sciences of the United States of America*, *75*(10), 4828–4832. https://doi.org/10.1073/pnas.75.10.4828

Datsenko, K. A., & Wanner, B. L. (2000). One-step inactivation of chromosomal genes in Escherichia coli K-12 using PCR products. *Proceedings of the National Academy of Sciences of the United States of America*, *97*(12), 6640–6645. https://doi.org/10.1073/pnas.120163297

Dong, H., & Kurland, C. G. (1995). Ribosome mutants with altered accuracy translate with reduced processivity. *Journal of Molecular Biology*, *248*(3), 551–561. https://doi.org/10.1006/jmbi.1995.0242

Durão, P., Balbontín, R., & Gordo, I. (2018). Evolutionary Mechanisms Shaping the Maintenance of Antibiotic Resistance. *Trends in Microbiology*, *26*(8), 677–691. https://doi.org/10.1016/j.tim.2018.01.005

Durão, P., Trindade, S., Sousa, A., & Gordo, I. (2015). Multiple Resistance at No Cost: Rifampicin and Streptomycin a Dangerous Liaison in the Spread of Antibiotic Resistance. *Molecular Biology and Evolution*, *32*(10), 2675–2680. https://doi.org/10.1093/molbev/msv143

Dutta, D., Shatalin, K., Epshtein, V., Gottesman, M. E., & Nudler, E. (2011). Linking RNA polymerase backtracking to genome instability in E. coli. *Cell*, *146*(4), 533–543. https://doi.org/10.1016/j.cell.2011.07.034

Figueroa-Bossi, N., & Bossi, L. (2015). Recombineering applications for the mutational analysis of bacterial RNA-binding proteins and their sites of action. *Methods in Molecular Biology (Clifton, N.J.)*, *1259*, 103–116. https://doi.org/10.1007/978-1-4939-2214-7_7

Fisher, R. F., & Yanofsky, C. (1983). Mutations of the beta subunit of RNA polymerase alter both transcription pausing and transcription termination in the trp operon leader region in vitro. *The Journal of Biological Chemistry*, *258*(13), 8146–8150.

Galas, D. J., & Branscomb, E. W. (1976). Ribosome slowed by mutation to streptomycin resistance. *Nature*, *262*(5569), 617–619. https://doi.org/10.1038/262617b0

Gartner, T. K., & Orias, E. (1966). Effects of mutations to streptomycin resistance on the rate of translation of mutant genetic information. *Journal of Bacteriology*, *91*(3), 1021–1028.

Global antimicrobial resistance surveillance system (GLASS) report: Early implementation 2017-2018. Geneva: World Health Organization. 2018. (n.d.).

Gorini, L., & Kataja, E. (1964). STREPTOMYCIN-INDUCED OVERSUPPRESSION IN E. COLI. *Proceedings of the National Academy of Sciences of the United States of America*, *51*, 995–1001. https://doi.org/10.1073/pnas.51.6.995

Gowrishankar, J., & Pittard, J. (1982). Regulation of phenylalanine biosynthesis in Escherichia coli K-12: Control of transcription of the pheA operon. *Journal of Bacteriology*, *150*(3), 1130–1137.

Guarente, L. P., & Beckwith, J. (1978). Mutant RNA polymerase of Escherichia coli terminates transcription in strains making defective rho factor. *Proceedings of the National Academy of Sciences of the United States of America*, *75*(1), 294–297. https://doi.org/10.1073/pnas.75.1.294

Gupta, R., Chatterjee, D., Glickman, M. S., & Shuman, S. (2017). Division of labor among Mycobacterium smegmatis RNase H enzymes: RNase H1 activity of RnhA or RnhC is essential for growth whereas RnhB and RnhA guard against killing by hydrogen peroxide in stationary phase. *Nucleic Acids Research*, *45*(1), 1–14. https://doi.org/10.1093/nar/gkw1046

Hall, A. R. (2013). Genotype-by-environment interactions due to antibiotic resistance and adaptation in Escherichia coli. *Journal of Evolutionary Biology*, *26*(8), 1655–1664. https://doi.org/10.1111/jeb.12172

Hall, Alex R., Iles, J. C., & MacLean, R. C. (2011). The fitness cost of rifampicin resistance in Pseudomonas aeruginosa depends on demand for RNA polymerase. *Genetics*, *187*(3), 817–822. https://doi.org/10.1534/genetics.110.124628

Hammer, K., Jensen, K. F., Poulsen, P., Oppenheim, A. B., & Gottesman, M. (1987). Isolation of Escherichia coli rpoB mutants resistant to killing by lambda cII protein and altered in pyrE gene attenuation. *Journal of Bacteriology*, *169*(11), 5289–5297. https://doi.org/10.1128/jb.169.11.5289-5297.1987

Herbert, K. M., Zhou, J., Mooney, R. A., Porta, A. L., Landick, R., & Block, S. M. (2010). E. coli NusG inhibits backtracking and accelerates pause-free transcription by promoting forward translocation of RNA polymerase. *Journal of Molecular Biology*, *399*(1), 17–30. https://doi.org/10.1016/j.jmb.2010.03.051

Hershberg, R. (2017). Antibiotic-Independent Adaptive Effects of Antibiotic Resistance Mutations. *Trends in Genetics: TIG*, *33*(8), 521–528. https://doi.org/10.1016/j.tig.2017.05.003

Hosaka, T., Tamehiro, N., Chumpolkulwong, N., Hori-Takemoto, C., Shirouzu, M., Yokoyama, S., & Ochi, K. (2004). The novel mutation K87E in ribosomal protein S12 enhances protein synthesis activity during the late growth phase in Escherichia coli. *Molecular Genetics and Genomics: MGG*, *271*(3), 317–324. https://doi.org/10.1007/s00438-004-0982-z

Jin, D. J., Cashel, M., Friedman, D. I., Nakamura, Y., Walter, W. A., & Gross, C. A. (1988). Effects of rifampicin resistant rpoB mutations on antitermination and interaction with nusA in Escherichia coli. *Journal of Molecular Biology*, *204*(2), 247–261. https://doi.org/10.1016/0022-2836(88)90573-6

Jin, D. J., & Gross, C. A. (1989). Characterization of the pleiotropic phenotypes of rifampin-resistant rpoB mutants of Escherichia coli. *Journal of Bacteriology*, *171*(9), 5229–5231. https://doi.org/10.1128/jb.171.9.5229-5231.1989

Jin, D. J., & Gross, C. A. (1991). RpoB8, a rifampicin-resistant termination-proficient RNA polymerase, has an increased Km for purine nucleotides during transcription elongation. *The Journal of Biological Chemistry*, *266*(22), 14478–14485.

Jin, D. J., Walter, W. A., & Gross, C. A. (1988). Characterization of the termination phenotypes of rifampicin-resistant mutants. *Journal of Molecular Biology*, *202*(2), 245–253. https://doi.org/10.1016/0022-2836(88)90455-x

Jin, D. J., & Zhou, Y. N. (1996). Mutational analysis of structure-function relationship of RNA polymerase in Escherichia coli. *Methods in Enzymology*, *273*, 300–319. https://doi.org/10.1016/s0076-6879(96)73027-6

Katz, S., & Hershberg, R. (2013). Elevated mutagenesis does not explain the increased frequency of antibiotic resistant mutants in starved aging colonies. *PLoS Genetics*, *9*(11), e1003968. https://doi.org/10.1371/journal.pgen.1003968

Kim, J., Yoon, J., Ju, M., Lee, Y., Kim, T.-H., Kim, J., … Han, S.-J. (2013). Identification of two HIV inhibitors that also inhibit human RNaseH2. *Molecules and Cells*, *36*(3), 212–218. https://doi.org/10.1007/s10059-013-2348-z

Kogoma, T. (1997). Stable DNA replication: Interplay between DNA replication, homologous recombination, and transcription. *Microbiology and Molecular Biology Reviews: MMBR*, *61*(2), 212–238.

Kohler, R., Mooney, R. A., Mills, D. J., Landick, R., & Cramer, P. (2017). Architecture of a transcribing-translating expressome. *Science (New York, N.Y.)*, *356*(6334), 194–197. https://doi.org/10.1126/science.aal3059

Lang, K. S., Hall, A. N., Merrikh, C. N., Ragheb, M., Tabakh, H., Pollock, A. J., … Merrikh, H. (2017). Replication-Transcription Conflicts Generate R-Loops that Orchestrate Bacterial Stress Survival and Pathogenesis. *Cell*, *170*(4), 787-799.e18. https://doi.org/10.1016/j.cell.2017.07.044

Lennox, E. S. (1955). Transduction of linked genetic characters of the host by bacteriophage P1. *Virology*, *1*(2), 190–206. https://doi.org/10.1016/0042-6822(55)90016-7

Li, X.-T., Thomason, L. C., Sawitzke, J. A., Costantino, N., & Court, D. L. (2013). Positive and negative selection using the tetA-sacB cassette: Recombineering and P1 transduction in Escherichia coli. *Nucleic Acids Research*, *41*(22), e204. https://doi.org/10.1093/nar/gkt1075

Lin, L. L., & Little, J. W. (1988). Isolation and characterization of noncleavable (Ind-) mutants of the LexA repressor of Escherichia coli K-12. *Journal of Bacteriology*, *170*(5), 2163–2173. https://doi.org/10.1128/jb.170.5.2163-2173.1988

Maniatis et al. Molecular cloning: A laboratory manual (CSHL Press). (n.d.).

Maslowska, K. H., Makiela-Dzbenska, K., & Fijalkowska, I. J. (2019). The SOS system: A complex and tightly regulated response to DNA damage. *Environmental and Molecular Mutagenesis*, *60*(4), 368–384. https://doi.org/10.1002/em.22267

McMahon, G., & Landau, J. V. (1982). Effect of S12 ribosomal mutations on peptide chain elongation in Escherichia coli: A hydrostatic pressure study. *Journal of Bacteriology*, *151*(1), 516–520.

Merrikh, H., Machón, C., Grainger, W. H., Grossman, A. D., & Soultanas, P. (2011). Co-directional replication-transcription conflicts lead to replication restart. *Nature*, *470*(7335), 554–557. https://doi.org/10.1038/nature09758

Merrikh, H., Zhang, Y., Grossman, A. D., & Wang, J. D. (2012). Replication-transcription conflicts in bacteria. *Nature Reviews. Microbiology*, *10*(7), 449–458. https://doi.org/10.1038/nrmicro2800

Minias, A. E., Brzostek, A. M., Korycka-Machala, M., Dziadek, B., Minias, P., Rajagopalan, M., … Dziadek, J. (2015). RNase HI Is Essential for Survival of Mycobacterium smegmatis. *PloS One*, *10*(5), e0126260. https://doi.org/10.1371/journal.pone.0126260

Moura de Sousa, J., Balbontín, R., Durão, P., & Gordo, I. (2017). Multidrug-resistant bacteria compensate for the epistasis between resistances. *PLoS Biology*, *15*(4), e2001741. https://doi.org/10.1371/journal.pbio.2001741

Murphy, K. C., Campellone, K. G., & Poteete, A. R. (2000). PCR-mediated gene replacement in Escherichia coli. *Gene*, *246*(1–2), 321–330. https://doi.org/10.1016/s0378-1119(00)00071-8

Negro, V., Krin, E., Aguilar Pierlé, S., Chaze, T., Giai Gianetto, Q., Kennedy, S. P., … Baharoglu, Z. (2019). RadD Contributes to R-Loop Avoidance in Sub-MIC Tobramycin. *MBio*, *10*(4). https://doi.org/10.1128/mBio.01173-19

Ochi, K., & Hosaka, T. (2013). New strategies for drug discovery: Activation of silent or weakly expressed microbial gene clusters. *Applied Microbiology and Biotechnology*, *97*(1), 87–98. https://doi.org/10.1007/s00253-012-4551-9

Ozaki, M., Mizushima, S., & Nomura, M. (1969). Identification and functional characterization of the protein controlled by the streptomycin-resistant locus in E. coli. *Nature*, *222*(5191), 333–339. https://doi.org/10.1038/222333a0

Paulander, W., Maisnier-Patin, S., & Andersson, D. I. (2009). The fitness cost of streptomycin resistance depends on rpsL mutation, carbon source and RpoS (sigmaS). *Genetics*, *183*(2), 539–546, 1SI-2SI. https://doi.org/10.1534/genetics.109.106104

Pelchovich, G., Nadejda, S., Dana, A., Tuller, T., Bravo, I. G., & Gophna, U. (2014). Ribosomal mutations affecting the translation of genes that use non-optimal codons. *The FEBS Journal*, *281*(16), 3701–3718. https://doi.org/10.1111/febs.12892

Proshkin, S., Rahmouni, A. R., Mironov, A., & Nudler, E. (2010). Cooperation between translating ribosomes and RNA polymerase in transcription elongation. *Science (New York, N.Y.)*, *328*(5977), 504–508. https://doi.org/10.1126/science.1184939

Qi, Q., Preston, G. M., & MacLean, R. C. (2014). Linking system-wide impacts of RNA polymerase mutations to the fitness cost of rifampin resistance in Pseudomonas aeruginosa. *MBio*, *5*(6), e01562. https://doi.org/10.1128/mBio.01562-14

Quillardet, P., Huisman, O., D'Ari, R., & Hofnung, M. (1982). SOS chromotest, a direct assay of induction of an SOS function in Escherichia coli K-12 to measure genotoxicity. *Proceedings of*

the National Academy of Sciences of the United States of America, *79*(19), 5971–5975. https://doi.org/10.1073/pnas.79.19.5971

Quiñones, A., Kücherer, C., Piechocki, R., & Messer, W. (1987). Reduced transcription of the rnh gene in Escherichia coli mutants expressing the SOS regulon constitutively. *Molecular & General Genetics: MGG*, *206*(1), 95–100. https://doi.org/10.1007/bf00326542

Reynolds, M. G. (2000). Compensatory evolution in rifampin-resistant Escherichia coli. *Genetics*, *156*(4), 1471–1481.

Ruusala, T., Andersson, D., Ehrenberg, M., & Kurland, C. G. (1984). Hyper-accurate ribosomes inhibit growth. *The EMBO Journal*, *3*(11), 2575–2580.

Saxena, S., Myka, K. K., Washburn, R., Costantino, N., Court, D. L., & Gottesman, M. E. (2018). Escherichia coli transcription factor NusG binds to 70S ribosomes. *Molecular Microbiology*, *108*(5), 495–504. https://doi.org/10.1111/mmi.13953

Schrag, S. J., & Perrot, V. (1996). Reducing antibiotic resistance. *Nature*, *381*(6578), 120–121. https://doi.org/10.1038/381120b0

Sedlyarova, N., Rescheneder, P., Magán, A., Popitsch, N., Rziha, N., Bilusic, I., … Nudler, E. (2017). Natural RNA Polymerase Aptamers Regulate Transcription in E. coli. *Molecular Cell*, *67*(1), 30-43.e6. https://doi.org/10.1016/j.molcel.2017.05.025

Shee, C., Cox, B. D., Gu, F., Luengas, E. M., Joshi, M. C., Chiu, L.-Y., … Rosenberg, S. M. (2013). Engineered proteins detect spontaneous DNA breakage in human and bacterial cells. *ELife*, *2*, e01222. https://doi.org/10.7554/eLife.01222

Stockum, A., Lloyd, R. G., & Rudolph, C. J. (2012). On the viability of Escherichia coli cells lacking DNA topoisomerase I. *BMC Microbiology*, *12*, 26. https://doi.org/10.1186/1471-2180-12-26

Subramaniam, A. R., Pan, T., & Cluzel, P. (2013). Environmental perturbations lift the degeneracy of the genetic code to regulate protein levels in bacteria. *Proceedings of the National Academy of*

Sciences of the United States of America, *110*(6), 2419–2424. https://doi.org/10.1073/pnas.1211077110

Tadokoro, T., & Kanaya, S. (2009). Ribonuclease H: Molecular diversities, substrate binding domains, and catalytic mechanism of the prokaryotic enzymes. *The FEBS Journal*, *276*(6), 1482–1493. https://doi.org/10.1111/j.1742-4658.2009.06907.x

Tramontano, E., Corona, A., & Menendez-Arias, L. (2019). Ribonuclease H, an unexploited target for antiviral intervention against HIV and hepatitis B virus. *Antiviral Research*, 104613. https://doi.org/10.1016/j.antiviral.2019.104613

Trindade, S., Sousa, A., & Gordo, I. (2012). Antibiotic resistance and stress in the light of Fisher's model. *Evolution; International Journal of Organic Evolution*, *66*(12), 3815–3824. https://doi.org/10.1111/j.1558-5646.2012.01722.x

Trindade, S., Sousa, A., Xavier, K. B., Dionisio, F., Ferreira, M. G., & Gordo, I. (2009). Positive epistasis drives the acquisition of multidrug resistance. *PLoS Genetics*, *5*(7), e1000578. https://doi.org/10.1371/journal.pgen.1000578

Vogwill, T., & MacLean, R. C. (2015). The genetic basis of the fitness costs of antimicrobial resistance: A meta-analysis approach. *Evolutionary Applications*, *8*(3), 284–295. https://doi.org/10.1111/eva.12202

Wang, C. H., & Koch, A. L. (1978). Constancy of growth on simple and complex media. *Journal of Bacteriology*, *136*(3), 969–975.

Wimberly, H., Shee, C., Thornton, P. C., Sivaramakrishnan, P., Rosenberg, S. M., & Hastings, P. J. (2013). R-loops and nicks initiate DNA breakage and genome instability in non-growing Escherichia coli. *Nature Communications*, *4*, 2115. https://doi.org/10.1038/ncomms3115

Wrande, M., Roth, J. R., & Hughes, D. (2008). Accumulation of mutants in "aging" bacterial colonies is due to growth under selection, not stress-induced mutagenesis. *Proceedings of the National*

Academy of Sciences of the United States of America, *105*(33), 11863–11868. https://doi.org/10.1073/pnas.0804739105

Yanofsky, C., & Horn, V. (1981). Rifampin resistance mutations that alter the efficiency of transcription termination at the tryptophan operon attenuator. *Journal of Bacteriology*, *145*(3), 1334–1341.

Yu, D., Ellis, H. M., Lee, E. C., Jenkins, N. A., Copeland, N. G., & Court, D. L. (2000). An efficient recombination system for chromosome engineering in Escherichia coli. *Proceedings of the National Academy of Sciences of the United States of America*, *97*(11), 5978–5983. https://doi.org/10.1073/pnas.100127597

Zaman, S., Fitzpatrick, M., Lindahl, L., & Zengel, J. (2007). Novel mutations in ribosomal proteins L4 and L22 that confer erythromycin resistance in Escherichia coli. *Molecular Microbiology*, *66*(4), 1039–1050. https://doi.org/10.1111/j.1365-2958.2007.05975.x

Zhou, Y. N., & Jin, D. J. (1997). RNA polymerase beta mutations have reduced sigma70 synthesis leading to a hyper-temperature-sensitive phenotype of a sigma70 mutant. *Journal of Bacteriology*, *179*(13), 4292–4298. https://doi.org/10.1128/jb.179.13.4292-4298.1997

Zhou, Y. N., & Jin, D. J. (1998). The rpoB mutants destabilizing initiation complexes at stringently controlled promoters behave like “stringent” RNA polymerases in Escherichia coli. *Proceedings of the National Academy of Sciences of the United States of America*, *95*(6), 2908–2913. https://doi.org/10.1073/pnas.95.6.2908

Zhou, Yan Ning, Lubkowska, L., Hui, M., Court, C., Chen, S., Court, D. L., … Kashlev, M. (2013). Isolation and characterization of RNA polymerase rpoB mutations that alter transcription slippage during elongation in Escherichia coli. *The Journal of Biological Chemistry*, *288*(4), 2700–2710. https://doi.org/10.1074/jbc.M112.429464